



Estimation of expected human attention weights based on a decision field theory model



Andres G. Abad^a, Jionghua (Judy) Jin^{b,*}, Young-Jun Son^c

^a Escuela Superior Politecnica del Litoral (ESPOL), Guayaquil, Ecuador

^b Department of Industrial and Operations Engineering, University of Michigan, Ann Arbor, MI, USA

^c Department of Systems and Industrial Engineering, The University of Arizona, Tucson, AZ, USA

ARTICLE INFO

Article history:

Received 3 December 2009

Received in revised form 22 March 2011

Accepted 8 March 2014

Available online 27 March 2014

Keywords:

Decision field theory

Decision making

Dynamic deliberation process

Attention weight

Sequential estimation

Adaptive learning

ABSTRACT

Modeling human decision making behavior is of great interest in understanding how a decision maker weights different decision attributes when making a decision. Such knowledge is critically important in helping predict future decisions, evaluating human decision performance, and improving the design of human and machine interface systems. Decision field theory (DFT) provides a psychological representation of the cognitive deliberation process, which is driven by the fluctuations of a person's attention among decision attributes. In this research area, the most common use of a DFT model is to estimate or predict the human decisions by using a set of pre-specified expected attention weights (EAWs) in the DFT model. Unlike other research, this paper extends the capabilities of DFT in a complementary direction, showing how to fit or train a DFT model by estimating the EAW based on sequentially obtained samples of decision trials. Furthermore, the inherent connection between the EAW and the decision choice uncertainty is investigated. The proposed modeling method is discussed in detail for a two-alternative decision scenario based on two attributes. Both simulations and a case study are conducted in the paper to demonstrate the effectiveness of the proposed modeling approach.

© 2014 Elsevier Inc. All rights reserved.

1. Introduction

There is an increasing research interest in understanding human decision making behavior, evaluating human decision making performance, and assisting human beings in making decisions. Accurate modeling of human decision making behavior will improve the prediction of future decisions, provide increasingly effective designs of human–machine interfaces, and guide the training of expert systems, and so on. As a fundamental requirement, an effective decision making model should be able to adequately represent the decision maker's historical decision behavior and reliably predict future decisions.

The research of decision making modeling is of a multidisciplinary nature and has been investigated in many different contexts. Townsend and Busemeyer [20] introduced a dynamic decision making model called decision field theory (DFT). Decision field theory belongs to a large class of models called sequential sampling models; information about these models is found in [14,16,21]. Because of the dynamic nature of the model, DFT has been successfully used to model various dynamic decision making scenarios, including an operator's reliance on automation in [8,9], dynamic route guidance in [19], and a broker's behavior in a virtual stock market in [13]. Recently, a comprehensive study was conducted in [12] to compare

* Corresponding author. Tel.: +1 734 763 0519; fax: +1 734 764 3451.

E-mail address: jhjin@umich.edu (J. (Judy) Jin).

the DFT model with another cognitive preferential choice model called the proportional difference (PD) model [11], in terms of the ability to predict people's decisions in nondominated gambling scenarios. The study showed that the DFT models were more accurate in predicting people's decisions than the PD models under the investigated scenario.

The DFT model provides a useful framework for modeling human decision behavior, particularly considering the dynamic and sequential aspects of decision making under conditions of uncertainty or risk. A key parameter affecting the model's performance and its ability to accurately predict decisions, is the estimated expected attention weight (EAW), which reflects the degree of attentions allocated to each attribute considered in the course of decision-making [18]. Due to the random nature of the attention weights, the DFT model is inherently a probabilistic model describing the choice preferences of a decision maker [17]. Which can provide different decision probabilities for each alternative. In this way, DFT model differentiates from the classical weighted utility models [2] in that the (attention) weights in DFT are stochastic, thus considering these weights in terms of their expected value is necessary.

In most of the literature, the EAW is pre-specified and the resulting model is used to predict the future decision-making behavior of a given subject. Unlike other research, this paper extends the capabilities of DFT in a complementary direction, showing how to fit or train a DFT model by estimating the EAW on the basis of an individual's ongoing decision behavior in the task. In this way, the proposed method can be considered as a way to adaptively characterize a subject's decision-making behavior based on his/her sequential decisions. Furthermore, the proposed method can also be used as a way to adaptively predict the subject's future decisions by utilizing the adaptively estimated EAW.

Generally, the fitting and training of a DFT model is achieved through a high dimensional search of the optimal model parameters, aimed to minimize the sum of the squared deviations between real values and predicted values. For example, in [5], the search was done over the squared deviations of the response time (time to arrive to a decision) for estimating seven model parameters. In [6], the model parameters were obtained by minimizing the deviations between the choice probabilities and the predicted ones. In [3,4], the same estimation approach is employed, using the FMINSEARCH routine of MATLAB. Differently from those existing approaches, this paper is to develop a new adaptive estimation method for estimating the EAW parameter based on sequential decision trials. With the adaptive estimation capability, the proposed method can efficiently capture a change of the subject's attention weights along his/her sequential decisions, which can further improve the DFT model performance in predicting the subject's future decisions.

The rest of the paper is structured as follows: Section 2 introduces the concepts of macro and micro-decision processes together with a brief review of the DFT model. Section 3 provides the proposed modeling framework in which a new representation of the attribute measures (ΔM plane) along with the basic estimation principles are presented for a decision scenario with two alternatives based on two attributes. Section 4 discusses the details of our DFT modeling approach, where an adaptive estimation of the EAW is developed based on the sequentially obtained attribute measurements and decision trials. In Section 5, two simulations are conducted to illustrate the procedures of the sequential estimation algorithm and demonstrate its adaptive capability under the change of the EAW. In addition to the simulations, a real case study involving a human in the loop experiment is also conducted to validate the effectiveness of the proposed method. Conclusions are given in Section 6. Finally, future research directions are provided in Section 7.

2. Definition of time scales and review of DFT

2.1. Definition of time scales

Before discussing the detail of the proposed estimation method, we first need to introduce the two time scales to be used in the modeling. The symbol Δ is used to denote the sampling time interval of attribute measures, during which a decision has to be made before the next sampling of attribute measures. Therefore, the EAW is used to describe the average effect of a stochastic attention weight during decision interval Δ , in which a decision maker generates the competitive preference (valence) on different alternatives [18]. In this work, we assume that the EAW can either be the same or different for different decisions.

Based on the DFT modeling mechanism, each decision interval Δ may include multiple steps of deliberations with a shorter interval δ ($\Delta > \delta$). As shown in Fig. 1, the deliberation step $j = 0, 1, 2, \dots, N_D$ forms a micro-process within each decision interval Δ , with $N_D = \lfloor \Delta/\delta \rfloor$ denoting the maximum deliberation step for each decision. Therefore, $t_{ij} = i \cdot \Delta + k \cdot \delta$ is a general representation of any moment for decision i at deliberation step j . For simplifying the notation, we will refer to $t_{i,0}$ by t_i when it clearly represents each sampling time for obtaining attribute measurements at $t_{i,0}$. In addition, it is assumed that $t_{i,N_D} \leq t_{i+1}$. As shown in Fig. 1, attribute measurements are updated at each sampling time t_i ($i = 1, 2, \dots$), which requires the decision maker to provide the corresponding decision within the sampling interval that equals the decision interval Δ . In contrast to the micro-deliberation process with the smaller deliberation interval δ , t_i forms a macro-process with the sampling interval Δ .

2.2. Review of DFT model

Before we discuss the development of the EAW estimation method, a brief review of the DFT model and the associated notations used in this paper will be given in this subsection. In DFT models [1], the cumulative preference vector corresponding

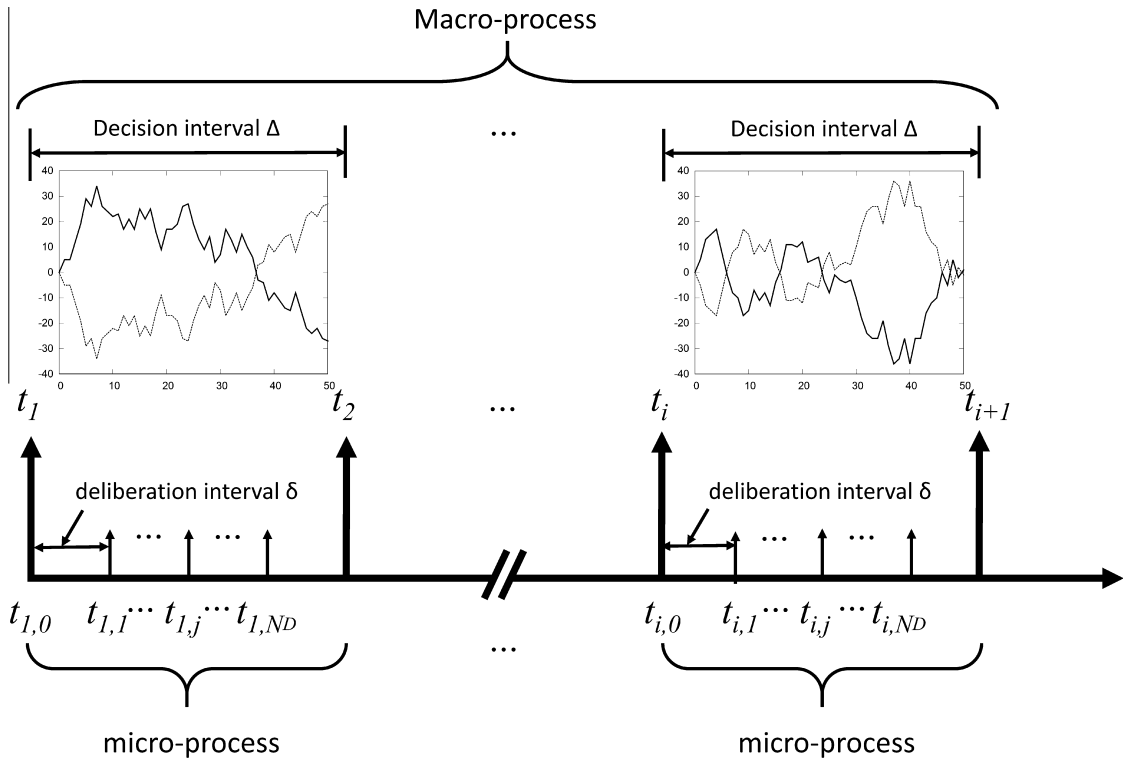


Fig. 1. Two different time scales for the micro and macro-processes.

to n alternatives at time $t_{i,j}$ is denoted as $P(t_{i,j}) = [p_1(t_{i,j}) \dots p_r(t_{i,j}) \dots p_n(t_{i,j})]^T$. There are two common rules for arriving to a decision in DFT. One rule is to choose alternative r at decision time t_{i,N_D} if $p_r(t_{i,N_D})$ is greater than all other elements $p_k(t_{i,N_D})$ for $k \neq r$. The other rule is to choose alternative r when $p_r(t_{i,j})$ is the first element exceeding a pre-specified preference threshold. When using this rule, the decision time may be different at different trials. In this paper, the former decision rule will be used under the fix decision time.

In DFT [1], the accumulated preference vector can be iteratively obtained as:

$$P(t_{i,j+1}) = S \cdot P(t_{i,j}) + V(t_{i,j+1}) \tag{1}$$

where S is an $n \times n$ matrix called the feedback matrix. In this paper, $S = \begin{bmatrix} \zeta & 0 \\ 0 & \zeta \end{bmatrix}$ with $|\zeta| < 1$. is used without considering the interactive feedback between two alternatives. $V(t_{i,j}) = [v_1(t_{i,j}) \ v_2(t_{i,j}) \ \dots \ v_n(t_{i,j})]^T$ is called valence column vector, and is formed by:

$$V(t_{i,j}) = C \cdot M(t_i) \cdot W(t_{i,j}). \tag{2}$$

C is called the contrast matrix. It is an $n \times n$ matrix used to compare all the alternatives between each other, and its elements are subjected to $\sum_{\forall q} c_{kq} = 0$ and $c_{kk} = 1$, with the following form:

$$C = \begin{bmatrix} 1 & -1/(n-1) & \dots & -1/(n-1) \\ -1/(n-1) & 1 & \dots & -1/(n-1) \\ \vdots & \vdots & \ddots & \vdots \\ -1/(n-1) & -1/(n-1) & \dots & 1 \end{bmatrix} \tag{3}$$

$M(t_i)$ is called the attribute matrix, and is an $n \times s$ matrix. At the i th decision, we will use the same $M(t_i)$ matrix for all the deliberation steps $j = 0, 1, \dots, N_D$, i.e., $M(t_{i,j}) = M(t_{i,j'}) = M(t_i)$. If each alternative has s attributes, the element $m_{rl}(t_i)$ of $M(t_i)$ corresponds to the measure of attribute l ($l = 1, \dots, s$) of alternative r ($r = 1, \dots, n$) obtained at time t_i and belonging to the i th macro-decision.

The column vector $W(t_{i,j} \in \mathfrak{R}^s)$ in (2) is called the attention weight vector. Each element of this vector is assumed to be independent Bernoulli random variables, i.e., $w_l(t_{i,j}) \sim \text{Bernoulli}(\rho_l(t_i))$, with $\rho_l(t_i) = E_j[w_l(t_{i,j})]$. It represents the amount of attention weight given to the l th attribute at time $t_{i,j}$. Note that the vector formed by $\rho_l(t_i)$ for ($l = 1, \dots, s$) is called the

EAW vector. This paper focuses on how to adaptively estimate $\rho(t_i)$ based on sequentially obtained attribute measures and human decisions.

3. Overview of modeling framework and estimation principles

3.1. Overview of modeling framework

The main purpose of this paper is to fit a DFT model by adaptively estimating the EAW parameter. In this way we can describe a decision maker’s behavior under sequential decision trials. Different from most of existing literature, this paper will extend the DFT model by considering a possible change of EAW when a decision maker faces different states of attribute measures at different times. Fig. 2 shows how this adaptive estimation approach is performed. For different samples of attribute measures, EAW is adaptively adjusted at the macro-process of time t_i to fit a DFT model that can predict the human decisions with the optimal matches of actual human’s sequential decisions. Because DFT employs the stochastic human attention weights at each deliberation time within a micro-process, it leads to a stochastic change of cumulative human preferences on different alternatives. Therefore, DFT can provide a quantitative justification of human decision uncertainty based on the probability of how the preference/confidence of the selected choice is competitive to that of other choices. In this way, DFT can provide a probabilistic risk assessment for all the possible choices. The detail of the estimation method will be discussed in Section 4.

3.2. Description of exemplary scenario and representation of probabilistic decisions

In this section we will illustrate the effect of EAW on the probability of human choices on two alternatives based on two attribute measures. Suppose we want to buy a car and there are two available car models to be chosen, based on two attributes: economy and quality. In this paper, the attribute matrix M is represented by continuous values with a standardized scale of $[0, 1]$. For example, the attribute matrix at time $t_{i,0}$ may be:

$$M(t_i) = \begin{matrix} & \begin{matrix} Economy & Quality \end{matrix} \\ \begin{bmatrix} 0.2 & 0.6 \\ 0.6 & 0.2 \end{bmatrix} & \begin{matrix} Car A \\ Car B \end{matrix} \end{matrix} \tag{4}$$

Fig. 3(a) shows two car models (alternatives) in the two dimensional attributes plane. In this scenario, it can be shown that the attribute differences between the two alternatives become a critical decision factor in DFT. These two attribute differences are given by:

$$\Delta m_1 = m_{11} - m_{21} = \text{Economy of Car A} - \text{Economy of Car B}$$

$$\Delta m_2 = m_{12} - m_{22} = \text{Quality of Car A} - \text{Quality of Car B}$$

In this paper the ΔM plane shown in Fig. 3(b), is proposed to better represent the attribute differences between two choices, where Δm_1 and Δm_2 are used as the horizontal axis and vertical axis, respectively. As a result, all decisions (points) in the ΔM plane can be clearly divided into two regions: one is called trivial decision region, with no uncertainty, and the other is called probabilistic decision region, with uncertainty. The following Axiom 1 describes how to make such a division.

Axiom 1. For a two-alternative decision scenario based on two attributes, the trivial decision region includes the first and third quadrants in the ΔM plane as shown in Fig. 3(b). Since $\Delta m_1 > 0$ and $\Delta m_2 > 0$ in quadrant 1 ($\Delta m_1 < 0$ and $\Delta m_2 < 0$ in quadrant 3), alternative A (alternative B) must be selected by any rational decision maker. In contrast, the probabilistic decision region covers the attributes in quadrants 2 and 4 in the ΔM plane, where the decision between two alternatives is made with a positive probability depending on the human attention weights over the two attributes.

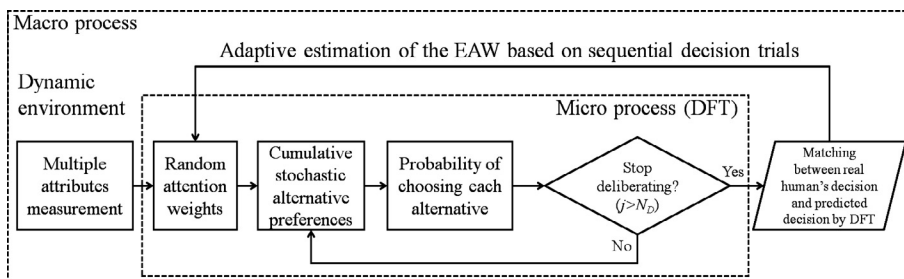


Fig. 2. Integrated framework for adaptive estimation of the EAW in DFT.

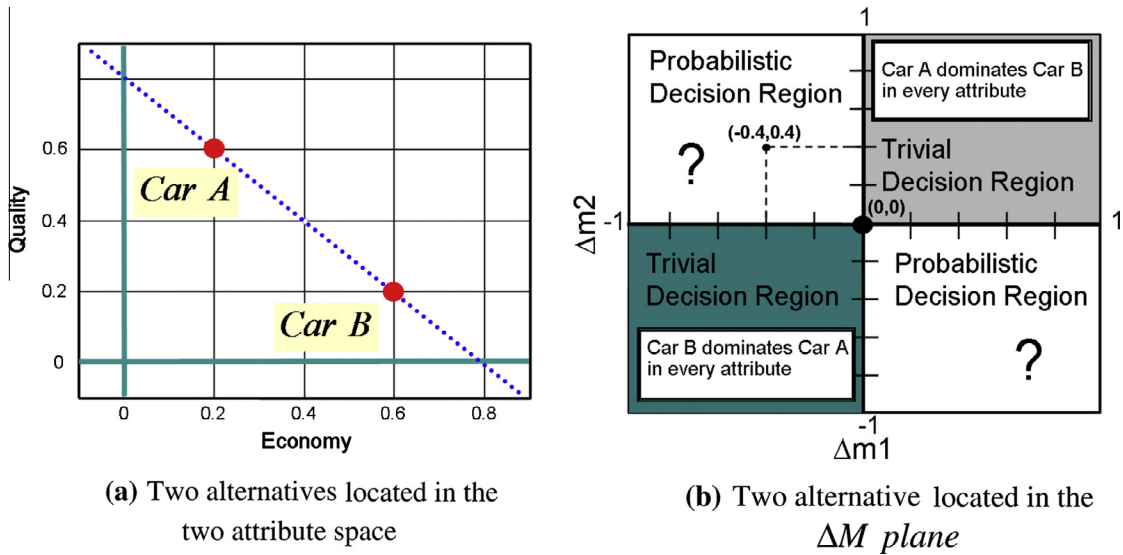


Fig. 3. Representation of attribute measures and division of decision regions.

Axiom 1 is easily explained in the above example of buying car A or car B. As shown in Fig. 3(b), if $(\Delta m_1, \Delta m_2)$ falls in quadrant 1 (quadrant 3), car A (car B) dominates car B (car A) in both quality and economy attributes, thus a decision is trivially determined. On the other hand, if $(\Delta m_1, \Delta m_2)$ falls in quadrant 2 (quadrant 4), car A dominates car B in quality (economy), while car B dominates car A in economy (quality). Consequently, the selection between car A and car B in the probabilistic decision region is determined by the person’s attention weight allocation between quality and economy. If a random attention weight is considered in the human deliberation process, a probabilistic decision is generated, which is modeled by DFT in this paper.

To fit a DFT model for a decision maker in the probabilistic decision region, the EAW vector $\rho(t_i) = [\rho_1(t_i) \cdots \rho_i(t_i) \cdots \rho_s(t_i)]^T$, which characterizes the Bernoulli random variables of human attentions given to each attribute at time $t_{i,j}$, is a key set of parameters to be estimated. Therefore, given $(\Delta m_1, \Delta m_2)$ in quadrants 2 and 4, the probability of choosing A, denoted as $Prob\{Choosing A\}$, is used to characterize the probabilistic uncertainty of decision A, which is calculated in the next subsection.

3.3. Calculation of choice probability

In order to obtain $Prob\{Choosing A\}$, based on (1), the distribution of stochastic preference is obtained iteratively by using a diffusion process approximation of DFT as:

$$P(t_{i,N_D}) = \sum_{0 \leq j \leq N_D - 1} S^j V(t_{i,n-j}) + S^{N_D} P(t_{i,0}) \tag{5}$$

The vector $P(t_{i,N_D})$ is a weighted sum of previous random valence vectors. As shown in (2), each of these valence vectors has the attention weight $W(t_{i,j})$ as one of its elements. Furthermore, each of the attention weight vectors follows a multivariate Bernoulli ($\rho(t_i)$) distribution. It is reasonably assumed that these random vectors are independent of each other. As a result, the distribution of $P(t_{i,N_D})$ converges into a multivariate normal distribution, i.e., $P(t_{i,N_D}) \sim Normal_n(\xi(t_{i,N_D}), \Phi(t_{i,N_D}))$, with the following mean and variance:

$$\xi(t_{i,N_D}) = [\zeta_A(t_{i,N_D}) \quad \zeta_B(t_{i,N_D})]^T = E[P(t_{i,N_D})] = [(I - S)^{-1}(I - S^{N_D}) \cdot C \cdot M(t_i)]\rho(t_i) + S^{N_D}P(t_{i,0}) \tag{6}$$

$$\Phi(t_{i,N_D}) = COV[P(t_{i,N_D})] = E\{[P(t_{i,N_D}) - \xi(t_{i,N_D})][P(t_{i,N_D}) - \xi(t_{i,N_D})]^T\} = \sum_{0 \leq j \leq N_D - 1} S^j (CM(t_i)COV[W(t_{i,N_D})]M(t_i)^T C^T) (S^j)^T \tag{7}$$

In the two-alternative scenario, $Prob\{Choosing A\}$ using DFT is equivalent to the probability of the preference of alternative A being higher than the preference of alternative B at the decision time t_{i,N_D} . Therefore, $Prob\{Choosing A\}$ is calculated by integrating the normal density function over $x_A > 0$ with $x^A = p_A(t_{i,N_D}) - p_B(t_{i,N_D})$, i.e.,

$$Prob\{Choosing A\} = \int_{x_A > 0} \exp[-(x_A - \delta_A)^2 / 2\lambda_A] / \sqrt{(2\pi\lambda_A)} dx_A \tag{8}$$

where $\delta_A = \zeta_A(t_{i,N_D}) - \zeta_B(t_{i,N_D})$, $\lambda_A = \varphi_{11}(t_{i,N_D}) + \varphi_{22}(t_{i,N_D}) - 2\varphi_{12}(t_{i,N_D})$, and φ_{ij} is the element in the i^{th} row and j^{th} column of the covariance matrix Φ in (7).

4. Estimation of EAW to fit a DFT model for a given decision maker

4.1. Relationship between decision boundary and EAW

Decision boundary (DB) is defined as the set of all ΔM plane points in the ΔM plane where alternative A and alternative B have an equal probability of being predicted by a fitted DFT. In other words, the DB is the set formed by all points in the ΔM plane where $Prob^{DFT}\{\text{Choosing A}\} = Prob^{DFT}\{\text{Choosing B}\} = 0.5$. **Theorem 1** formalizes the relationship between the DB and the EAW.

Theorem 1. *If the EAW is assumed to be constant across deliberations and based on DFT, the DB passes through the origin point (0, 0) and points $(\Delta m_1, \Delta m_2)$ in the ΔM plane satisfying $\frac{\Delta m_2}{\Delta m_1} = -\frac{\rho_1(t_i)}{1-\rho_1(t_i)}$, where $\rho_1(t_i) = E_j[w_1(t_{i,j})]$.*

Proof. It is not difficult to see why the DB passes through the origin point (0, 0). If we have to decide over two alternatives with the exact same attribute measures (which would be located at the origin point (0, 0)), we would have an equal likelihood of choosing any of these two alternatives regardless how much attention was given to each attribute.

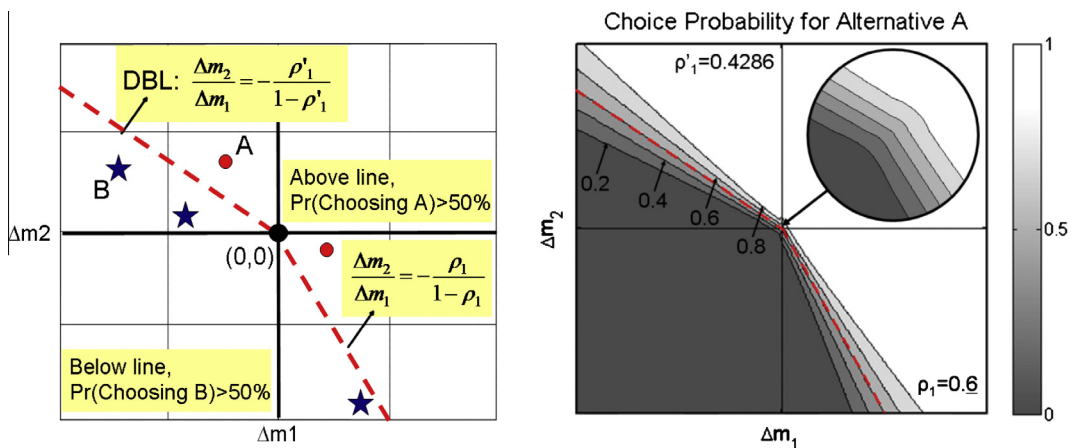
To prove that the other points $(\Delta m_1, \Delta m_2)$ in the DB must satisfy $\frac{\Delta m_2}{\Delta m_1} = -\frac{\rho_1(t_i)}{1-\rho_1(t_i)}$, we should remember that these points should satisfy the condition of having the preference on alternative A equal to the preference on alternative B at the decision time t_{i,N_D} , or equivalently $x_A = P_A(t_{i,N_D}) - P_B(t_{i,N_D}) = 0$. Based on (8), this condition will be satisfied if and only if $\delta_A = \zeta_A(t_{i,N_D}) - \zeta_B(t_{i,N_D}) = 0$. Based on (6), when $S = \begin{bmatrix} \zeta & 0 \\ 0 & \zeta \end{bmatrix}$ with $|\zeta| < 1$, $(I - S)^{-1}(I - S^{N_D})$ is a diagonal matrix with equal elements in the diagonal. Therefore, only the term $C \cdot M(t_i) \cdot \rho(t_i)$ needs to be considered to check $\delta_A = \zeta_A(t_{i,N_D}) - \zeta_B(t_{i,N_D}) = 0$. Since:

$$C \cdot M(t_i) \cdot \rho(t_i) = \begin{bmatrix} \rho_1(t_i)m_{11}(t_i) + \rho_2(t_i)m_{12}(t_i) - \rho_1(t_i)m_{21}(t_i) - \rho_2(t_i)m_{22}(t_i) \\ -\rho_1(t_i)m_{11}(t_i) - \rho_2(t_i)m_{12}(t_i) + \rho_1(t_i)m_{21}(t_i) + \rho_2(t_i)m_{22}(t_i) \end{bmatrix} = \begin{bmatrix} -\rho_1(t_i)\Delta m_1(t_i) - [1 - \rho_1(t_i)]\Delta m_2(t_i) \\ \rho_1(t_i)\Delta m_1(t_i) + [1 - \rho_1(t_i)]\Delta m_2(t_i) \end{bmatrix} \tag{9}$$

Then we need to have $-\rho_1(t_i)\Delta m_1(t_i) - [1 - \rho_1(t_i)]\Delta m_2(t_i) = \rho_1(t_i)\Delta m_1(t_i) + [1 - \rho_1(t_i)]\Delta m_2(t_i)$. Therefore, points in the DB must satisfy $\Delta m_2 = -\frac{\rho_1(t_i)}{1-\rho_1(t_i)} \Delta m_1$, and **Theorem 1** is proved. \square

Theorem 1 shows that under the assumption that the EAW remains constant over decision interval Δ , the DB is described by a line. Therefore, we can further call DB as decision boundary line (DBL). **Fig. 4** shows two examples of DBL lines in the ΔM plane, where the dot and star points correspond to human decisions on alternative A and alternative B respectively. The following **Proposition 1** is used to describe the corresponding choice probability limits.

Proposition 1. *Based on the definition of the DBL, the probability of choosing alternative A based on the DFT model should be higher than 50% for all the human decisions (dot points) above the DBL, while the probability of choosing alternative B based on the DFT model should be higher than 50% for all the human decisions (star points) below the DBL. If it is possible to find such a single EAW that the fitted DFT model can satisfy above condition, it is concluded that a DBL is existed, i.e., the decision maker may keep the constant EAW on the attributes to make all decisions up to the current decision.*



(a) Linear DBL in quadrants 2 and 4

(b) Predicted probability by DFT

Fig. 4. Linear decision boundary and probabilistic assessment.

It is worthwhile to notice that for two attributes, two Bernoulli random variables $w_1(t_{ij}) \sim \text{Bernoulli}(\rho_1(t_i))$ and $w_2(t_{ij}) \sim \text{Bernoulli}(\rho_2(t_i))$ are used to describe the random attention weight on each attribute at deliberation step j for decision i . We will further require that $\rho_2(t_i) = 1 - \rho_1(t_i)$ subjected to $0 \leq \rho_1(t_i) \leq 1$. In this case, DFT modeling only needs to estimate either $\rho_1(t_i)$ or $\rho_2(t_i)$. Therefore, in this paper we are only going to discuss the estimation of $\rho_1(t_i)$.

4.2. Fitting a DFT model to a decision maker

The decision maker behavior is characterized by all the decisions up to the current decision time. In this paper, for two alternatives, the decisions made by a decision maker and DFT will be represented as two vectors: $A^*(t_i) = [a_A^*(t_i) \ a_B^*(t_i)]^T$ and $\hat{A}(t_i) = [\hat{a}_A(t_i) \ \hat{a}_B(t_i)]^T$, in which $a_l^*(t_i) = \begin{cases} 1 & \text{alternative } l \text{ is chosen by decision maker} \\ 0 & \text{else} \end{cases}$ and $\hat{a}_l(t_i) = \begin{cases} 1 & \text{alternative } l \text{ is chosen by DFT} \\ 0 & \text{else} \end{cases}$ subjected to $\sum_{1 \leq l \leq n} a_l^*(t_i) = 1$ and $\sum_{1 \leq l \leq n} \hat{a}_l(t_i) = 1$, respectively. Therefore, the problem of fitting a DFT model for a decision maker can be reformulated as how to estimate $\rho_1(t_i)$ by solving the following optimization problem to ensure the best consistency between these two decision vectors.

$$\begin{aligned} \min_{\rho_1(t_i)} \quad & \sum_i d(a^*(t_i), \hat{a}(t_i)) \\ \text{s.t.} \quad & 0 \leq \rho_1(t_i) \leq 1 \end{aligned} \tag{10}$$

where $d(\cdot, \cdot)$ is a general distance metric function. Some often used distance metric functions include Euclidean distance, Hamming distance, and Mahalanobis distance. The detail comparisons of these distance metrics can be found in [7].

Based on Theorem 1, if the EAW is assumed to be constant over all decisions, i.e. $\rho_1(t_i) = \rho_1$, some searching algorithms can be used to find an optimal value of ρ_1 , that minimizes the objective function in (10). However, in general it is hard to guarantee a global minimum by using a searching algorithm. Moreover, since this paper mainly focuses on the sequential decisions scenario, it would be more interesting and efficient to develop an iterative adaptive estimation approach. For this purpose, Lemma 1 is given as follows to describe how to estimate the two limit lines for the DBL based on each sequentially obtained decision.

Lemma 1. Based on Proposition 1, when a DFT model is fitted to a decision maker, the corresponding DBL should fall between two limit lines: DBL^A and DBL^B , where DBL^A (DBL^B) is the line that links the origin point (0,0) and the boundary point of the decisions made by the decision maker on alternative A (on alternative B).

Fig. 5(a) shows how DBL^A and DBL^B are constructed, in which a dot point represents a real human decision A ($A^*(t_i) = [1 \ 0]^T$), and a star point represents a real human decision B ($A^*(t_i) = [0 \ 1]^T$). Based on Proposition 1, Fig. 5(a) also shows that the fitted DBL should fall between DBL^A and DBL^B to ensure the consistency between the real human decisions and the predicted decisions by DFT. As a result, the probability of choosing A by DFT model using such a DBL is higher than 50% for all dot points above DBL. A similar conclusion is obtained for all star points below DBL.

4.3. Estimation bounds of EAWs and choice probability

This subsection shows how the estimation bounds of the EAW can be obtained and how to interpret the resultant choice probability bounds.

Proposition 2. If $b^A(t_i)$ and $b^B(t_i)$ denote the corresponding slopes of DBL^A and DBL^B estimated at macro-scale time t_i , the corresponding two bounds $\rho_1^A(t_i)$ and $\rho_1^B(t_i)$ for ρ_1 can be obtained based on Proposition 1 and Lemma 1 as:

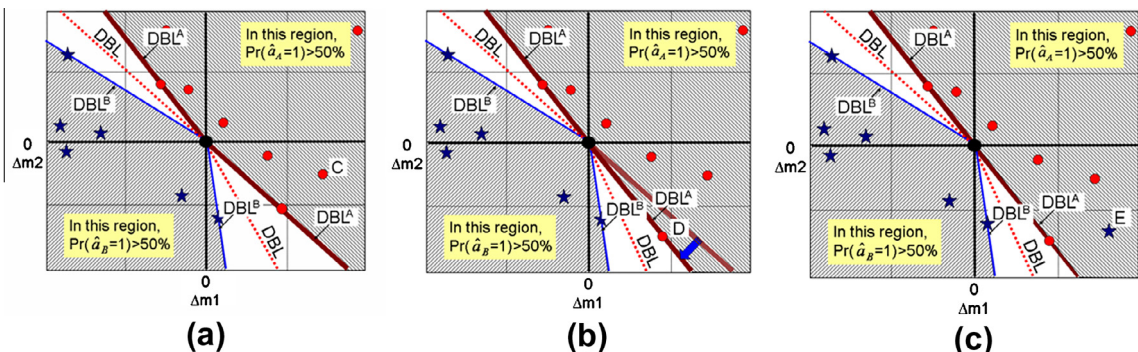


Fig. 5. Two limit lines of DBL and sequential updating principle.

$$\rho_1^A(t_i) = \frac{b^A(t_i)}{b^A(t_i) - 1} \quad \text{and} \quad \rho_1^B(t_i) = \frac{b^B(t_i)}{b^B(t_i) - 1} \tag{11}$$

Since the slopes $b^A(t_i)$ and $b^B(t_i)$ are negative, conditions $0 \leq \rho_1^A(t_i) \leq 1$ and $0 \leq \rho_1^B(t_i) \leq 1$ are satisfied. Next, Proposition 3 describes how choice probability bounds can be obtained by DFT using the bounds $\rho_1^A(t_i)$ and $\rho_1^B(t_i)$ respectively.

Proposition 3. When the estimated bounds $\rho_1^A(t_i)$ and $\rho_1^B(t_i)$ are used in the DFT model instead of the true, however unknown, parameter ρ_1 , the DFT model provides a corresponding lower and upper bound for the choice probability of alternative A. Similar bounds can be obtained for the choice probability on alternative B.

Based on Proposition 3, the following two equivalent conditions are held:

$$\begin{aligned} \text{(i)} \quad \text{Prob}_{\rho_1^A(t_i)}^{\text{DFT}} \{ \text{DFT choose A} | \text{real decision is A} \} &\leq \text{Prob}_{\rho_1}^{\text{DFT}} \{ \text{DFT choose A} | \text{real decision is A} \} \\ &\leq \text{Prob}_{\rho_1^B(t_i)}^{\text{DFT}} \{ \text{DFT choose A} | \text{real decision is A} \} \end{aligned} \tag{12}$$

$$\begin{aligned} \text{(ii)} \quad \text{Prob}_{\rho_1^B(t_i)}^{\text{DFT}} \{ \text{DFT choose B} | \text{real decision is B} \} &\leq \text{Prob}_{\rho_1}^{\text{DFT}} \{ \text{DFT choose B} | \text{real decision is B} \} \\ &\leq \text{Prob}_{\rho_1^A(t_i)}^{\text{DFT}} \{ \text{DFT choose B} | \text{real decision is B} \} \end{aligned} \tag{13}$$

Here, $\text{Prob}_{\rho_1^A(t_i)}^{\text{DFT}} \{ \text{DFT choose A} | \text{real decision is A} \}$ is used to denote the probability of choosing alternative A by DFT, using the EAW of $\rho_1^A(t_i)$ and under the condition that the human decision maker chose alternative A. Similar definitions are used for the other probabilities.

Proposition 3 can be explained by Fig. 5(a). For example, in quadrant 4, if the attribute measure point falls on DBL, the predicted probability of choosing A (or B) is 50% based on the DFT model with the true ρ_1 , while if the point is far above DBL, it leads to a higher probability of choosing A (higher than 50% based on Proposition 1). In contrast, when $\rho_1^A(t_i)$ ($\rho_1^B(t_i)$) is used in the DFT model instead of the true ρ_1 , the corresponding 50% probability decision line is artificially moved up (moved down) from true DBL to DBL^A (DBL^B). As a result, the given point C in Fig. 5(a) is located much less above DBL^A (much farther above DBL^B) than above DBL, which causes an under-estimation (over-estimation) of the probability of choosing A by using the DFT model with $\rho_1^A(t_i)$ ($\rho_1^B(t_i)$) corresponding to DBL^A (DBL^B). Therefore, $\text{Prob}_{\rho_1^A(t_i)}^{\text{DFT}} \{ \text{DFT choose A} | \text{real decision is A} \}$ and $\text{Prob}_{\rho_1^B(t_i)}^{\text{DFT}} \{ \text{DFT choose A} | \text{real decision is A} \}$ provide a lower and upper bound of $\text{Prob}_{\rho_1}^{\text{DFT}} \{ \text{DFT choose A} | \text{real decision is A} \}$, respectively. A similar interpretation can be given to the case of the real human decision on alternative B in (13).

4.4. Performance measure of estimated bounds of EAWs

Using Proposition 2, a way to obtain $\rho_1^A(t_i)$ and $\rho_1^B(t_i)$ based on the slopes b^A and b^B has been presented. Moreover, it would be desired to know whether such bounds, $\rho_1^A(t_i)$ and $\rho_1^B(t_i)$, are good enough for the fitted DFT model to predict future decisions. Therefore, a way of assessing the uncertainty imposed by these bounds to our estimator would be of great interest. For this purpose, based on (12) and (13), the following performance index is defined to describe the probabilistic uncertainty range of the decisions that are made by the estimated DFT model using the bounds of the EAW $\rho_1(t_i)^A$ and $\rho_1(t_i)^B$:

$$U(\Delta m_1, \Delta m_2) = \text{Prob}_{\rho_1^B(t_i)}^{\text{DFT}} \{ \text{DFT choose A} | \text{real decision is A} \} - \text{Prob}_{\rho_1^A(t_i)}^{\text{DFT}} \{ \text{DFT choose A} | \text{real decision is A} \}$$

or,

$$U(\Delta m_1, \Delta m_2) = \text{Prob}_{\rho_1^A(t_i)}^{\text{DFT}} \{ \text{DFT choose B} | \text{real decision is B} \} - \text{Prob}_{\rho_1^B(t_i)}^{\text{DFT}} \{ \text{DFT choose B} | \text{real decision is B} \} \tag{14}$$

$U(\Delta m_1, \Delta m_2)$ is defined as $U(x, y): \mathfrak{R}^2 \rightarrow [0, 1]$. If $U(x, y) \rightarrow 0$, the upper and lower bounds of the probability of choosing A or B by DFT converges. As a result, the estimation bounds of EAW also converges to the true ρ_1 . The average uncertainty measure index is defined as $\frac{1}{|ur|} \iint_{ur} U dA'$, where ur defines the uncertainty region, and $|ur|$ is equal to the area of the uncertainty region.

4.5. Estimation of slope bounds of DBL

In Section 4.2, Lemma 1 provides the principle of how to obtain DBL^A and DBL^B to match all available human decisions. However, a formal definition of the method has not been provided. This subsection presents how to find DBL^A and DBL^B mathematically by estimating b^A and b^B through an optimization formulation and how to adaptively update this estimation based on sequentially obtained decisions.

The following optimization problem is formalized based on the principle in Lemma 1, which intends to estimate b^A and b^B of DBL to match all available human decisions.

$$\begin{aligned}
& \max_{b^A, b^B} |b^A - b^B| \\
& \text{s.t. } \Delta m_2(t_i) \neq -\Delta m_1(t_i), \forall b \in (b^A, b^B) \text{ in quadrant 2, or } \forall b \in (b^B, b^A) \text{ in quadrant 4} \\
& \Delta m_2(t_i)[1 \ -1] \cdot [a_A^*(t_i) \ a_B^*(t_i)]^T \geq \Delta m_1(t_i) [b^A \ -b^B] \cdot [a_A^*(t_i) \ a_B^*(t_i)]^T
\end{aligned} \tag{15}$$

where $i = 1, 2, \dots$ indicates all available decisions at either quadrant 2 or 4. The first condition in (15) keeps all provided decisions outside the region defined by the two boundary lines DBL^A and DBL^B . The second condition keeps all human decisions belonging to alternative A ($[a_A^*(t_i) \ a_B^*(t_i)]^T = [1 \ 0]^T$) above DBL^A ($\Delta m_2 \geq b^A \Delta m_1$); while also keeping all human decisions belonging to alternative B ($[a_A^*(t_i) \ a_B^*(t_i)]^T = [0 \ 1]^T$) below DBL^B ($\Delta m_2 \leq b^B \Delta m_1$).

While the formulation of the problem provided in (15) is effective, it might not be efficient for applications with sequential decisions. For this reason, we have developed an iterative algorithm that is efficient to model the sequentially obtained decisions. Fig. 5(b) shows how DBL is updated when a new decision is available. When a new decision falls between the previously estimated DBL^A and DBL^B , the newly updated DBL^A or DBL^B should pass this newest boundary points if the decision maker chooses alternative A or alternative B, respectively. As shown in Fig. 5(b), DBL^A is adjusted to include this new sample of human decision A (dot point D). A flowchart for implementing this sequential estimation algorithm is given in Fig. 6.

It is worthwhile to note that DBL^A or DBL^B will only be updated if an incoming new point falls between DBL^A and DBL^B . However, it is possible to observe a conflict decision (e.g. an incoming new star point falling above DBL^A). As shown in Fig. 5(c), a star point E represents a real human decision on alternative B, but point E falls above DBL^A leading to the probability of choosing A higher than 50% by using the DFT model based on Proposition 1. It is then called a conflict point. If this conflict is not due to random decision uncertainty or human errors, it might indicate a change in the EAW. This case will be studied in Section 4.6.

4.6. Analysis of decision uncertainty and inconsistency

In the sequential decision making scenario, the performance feedback may sometimes be provided to decision makers for improving their future decision performance [10]. In this paper, we assume that such feedback may cause a decision maker

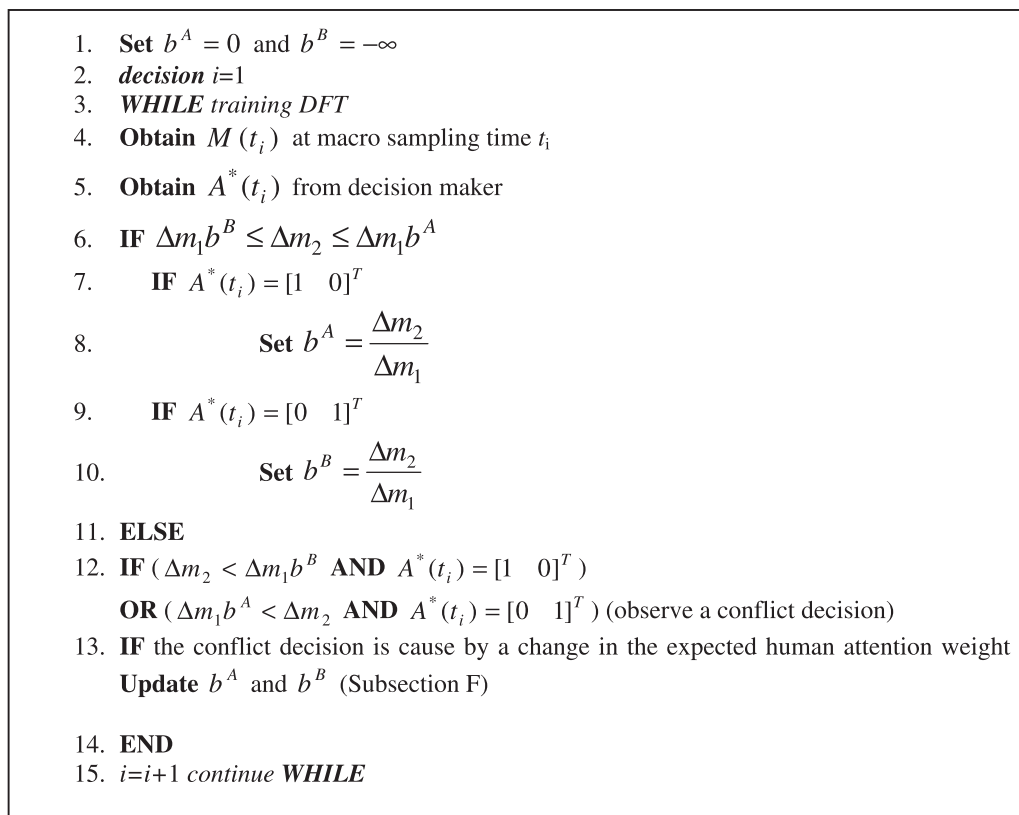


Fig. 6. Pseudocode for sequential estimation of DBL's slope bounds.

to make some shift on his/her EAWs in an attempt to improve future decisions. This shift of EAWs may lead to conflict decisions that are *probabilistically* inconsistent with those previously observed decisions under the un-shifted EAWs. On the other hand, a single inconsistent decision may also be due to random human decision errors. In this case, it is important to avoid over-fitting of a DFT model due to an inappropriate adjustment on EAWs. As shown in [15], a complex model may fit a data set well, but may not bear an interpretable relationship with the underlying mental process. This subsection discusses how to systematically judge whether an inconsistent decision is due to a change of human attention weights by assessing the likelihood of such a change.

An inconsistent decision is observed at time t_K if one of the following cases is held:

- (a) Under the real human decision A of $A^*(t_K) = [1 \ 0]^T$, the attribute measure $(\Delta m_1(t_K), \Delta m_2(t_K))$ is located below DBL^B , i.e., $\Delta m_2(t_K) < \Delta m_1(t_K)b^B$; or
- (b) Under the real human decision B of $A^*(t_K) = [0 \ 1]^T$, the attribute point $(\Delta m_1(t_K), \Delta m_2(t_K))$ is located above DBL^A , i.e., $\Delta m_2(t_K) > \Delta m_1(t_K)b^A$.

In order to justify whether an inconsistent decision is caused due to a change of human attention weights, or due to decision uncertainty or human errors, we compare the DFT predicted probabilities of generating the inconsistent decisions based on the previous estimation of $\rho_1^A(t_{K-1})$ or $\rho_1^B(t_{K-1})$ (assume no change occurs at t_K), with the predicted probabilities of the same decisions based on the new estimation of $\rho_1^A(t_K)$ or $\rho_1^B(t_K)$ (assume a change starts at t_K). In the following discussion, we will denote these two probability bounds by $P1$ and $P2$.

$P1$ is defined under the condition of the EAW has no change at t_K , which is the upper bound of the probability of generating this inconsistent human decision $A^*(t_K)$ by DFT using true ρ_1 , i.e., $P1 = Prob_{\rho_1^A(t_{K-1}) \text{ or } \rho_1^B(t_{K-1})}^{DFT} \{\hat{A}(t_K) = A^*(t_K)\} \geq Prob_{\rho_1}^{DFT} \{\hat{A}(t_K) = A^*(t_K)\}$. This probability can be computed by:

- (a) When the incoming real human decision A falls below DBL^B ,

$$P1 = Prob_{\rho_1^B(t_{K-1})}^{DFT} \{choose A \text{ at } (\Delta m_1(t_K), \Delta m_2(t_K)) | A^*(t_K) = [1 \ 0]^T; \Delta m_2(t_K) < \Delta m_1(t_K)b^B\}$$

- (b) When the incoming real human decision B falls above DBL^A ,

$$P1 = Prob_{\rho_1^A(t_{K-1})}^{DFT} \{choose B \text{ at } (\Delta m_1(t_K), \Delta m_2(t_K)) | A^*(t_K) = [0 \ 1]^T; \Delta m_2(t_K) > \Delta m_1(t_K)b^A\} \tag{16}$$

$P2$ is defined in (7) under the condition that the EAW changed at t_K . Based on the proposed algorithm (flowchart in Fig. 6), the slope bounds of DBL are updated at time t_K according to the real human decision $A^*(t_K)$ as follows:

- (a) For a real human decision $A^*(t_K) = [1 \ 0]^T$,

Set $b_{new}^A = \Delta m_2(t_K) / \Delta m_1(t_K)$ and

- (i) If $\Delta m_1(t_K) < 0, \Delta m_2(t_K) > 0$ (in quadrant 2), then $b_{new}^B = \min\{\Delta m_2(t_i) / \Delta m_1(t_i) | A^*(t_i) = [0 \ 1], \Delta m_2(t_i) < \Delta m_1(t_i)b_{new}^A, \forall i < K\}$.
- (ii) If $\Delta m_1(t_K) > 0, \Delta m_2(t_K) < 0$ (in quadrant 4), then $b_{new}^B = \max\{\Delta m_2(t_i) / \Delta m_1(t_i) | A^*(t_i) = [0 \ 1], \Delta m_2(t_i) < \Delta m_1(t_i)b_{new}^A, \forall i < K\}$

- (b) Similarly, for a real human decision $A^*(t_K) = [0 \ 1]^T$,

Set $b_{new}^B = \Delta m_2(t_K) / \Delta m_1(t_K)$ and

- (i) If $\Delta m_1(t_K) < 0, \Delta m_2(t_K) > 0$ (in quadrant 2), then $b_{new}^A = \max\{\Delta m_2(t_i) / \Delta m_1(t_i) | A^*(t_i) = [1 \ 0]; \Delta m_2(t_i) > \Delta m_1(t_i)b_{new}^B, \forall i < K\}$ or
- (ii) If $\Delta m_1(t_K) > 0, \Delta m_2(t_K) < 0$ (in quadrant 4), then $b_{new}^A = \min\{\Delta m_2(t_i) / \Delta m_1(t_i) | A^*(t_i) = [1 \ 0]; \Delta m_2(t_i) > \Delta m_1(t_i)b_{new}^B, \forall i < K\}$

After getting b_{new}^A and b_{new}^B , the corresponding bounds of $\rho_1^A(new)$ and $\rho_1^B(new)$ can be obtained based on Proposition 3. When $\rho_1^A(new)$ and $\rho_1^B(new)$ are used in the DFT model to predict the decisions for the old scenarios t_i ($1 \leq i < K$), it will generate some inconsistent decisions on old scenarios. The set of these inconsistent decisions will be denoted by Ω .

$P2$ is defined as the lower bound of the predicted probability of generating the Ω set by using $\rho_1^A(new)$ and $\rho_1^B(new)$ in the DFT model, i.e., $P2 = Prob_{\rho_1^A(new) \text{ or } \rho_1^B(new)}^{DFT} \{\hat{A}(t_i) \in \Omega\} \leq Prob_{\rho_1}^{DFT} \{\hat{A}(t_i) \in \Omega\}$. Since incoming decisions will be assumed to be independent of each other, these probabilities are calculated by:

(a) For a real decision A with $A^*(t_k) = [1 \ 0]^T$,

$$P2 = \prod_{0 \leq i < K} \text{Prob}_{\rho_1^A(\text{new})}^{\text{DFT}} \{ \text{choose B at } (\Delta m_1(t_i), \Delta m_2(t_i)) | A^*(t_i) = [0 \ 1]^T; \Delta m_2(t_i) > \Delta m_1(t_i) b_{\text{new}}^A; \forall i < k \}$$

(b) For a real decision B with $A^*(t_k) = [0 \ 1]^T$,

$$P2 = \prod_{0 \leq i < K} \text{Prob}_{\rho_1^B(\text{new})}^{\text{DFT}} \{ \text{choose A at } (\Delta m_1(t_i), \Delta m_2(t_i)) | A^*(t_i) = [1 \ 0]^T; \Delta m_2(t_i) < \Delta m_1(t_i) b_{\text{new}}^B; \forall i < K \} \tag{17}$$

Based on the probability bounds of P1 and P2, the following justification rule is used to determine whether the decision maker’s EAWs has changed or not.

Justification Rule: When an inconsistent decision is observed at time t_k , if $P2 > P1$, it is concluded that a change in the human EAWs has occurred. Otherwise, the inconsistent decision is due to the prediction uncertainty or decision errors.

5. Simulations and experimental case study

5.1. Case I: sequential estimation with constant EAWs

In Case I, we will use a simulation to demonstrate the proposed sequential estimation algorithm for estimating the bounds of EAWs. In this case, the EAW is assumed to be constant over all decisions. The simulated scenario corresponds to a two alternatives decision based on two attributes. Each of the two attributes is assumed to follow a uniform distribution over the range of $0 < \Delta m_1 < 1$ and $-1 < \Delta m_2 < 0$, respectively. In other words, each decision sample is located in quadrant 4 of the ΔM plane. To generate the alternative selected in each decision, a DFT model was used with an EAW of 0.6 on attribute 1. The simulated decisions are assumed to be available one by one sequentially. The DFT modeling is going to be done based on the generated sequential decisions and using the proposed algorithm shown in Fig. 6.

Fig. 7 depicts several exemplary steps of the sequential adjustment of the bounds of DBL. For example, $A^*(t_1) = [1 \ 0]^T$ (a dot point represents decision A) is used to obtain DBL^A at the first subfigure; and $A^*(t_2) = [1 \ 0]^T$ (a star point represents decision B) is used to obtain DBL^B at the second subfigure. However, there is no adjustment on DBL for $A^*(t_3) = [1 \ 0]^T$ because the attribute measures at t_3 of decision B (star point) is below DBL^B . Similarly, at the third subfigure, since the sample point (dot) at t_4 falls between DBL^A and DBL^B and $A^*(t_4) = [1 \ 0]^T$, a new adjustment on DBL^A is performed. This adjustment narrows further the bounds of DBL^A and DBL^B . The bottom three subfigures in Fig. 7 show how the bounds of DBL^A and DBL^B are continuously narrowed through the sequential adjustment of DBL^A or DBL^B at time t_9, t_{13} , and t_{37} respectively.

At each adjustment step of DBL^A or DBL^B , the corresponding bounds of the EAWs are obtained based on the estimated bounds of DBL^A and DBL^B . Fig. 8 shows how the estimation of $\rho_1^A(t_i)$ or $\rho_1^B(t_i)$ is narrowed over decision times and converges to the true value of $\rho_1 = 0.6$.

To further show the performance of the estimation bounds, the function $U(x, y)$ is calculated based on (14) by using $\rho_1^A(t_i)$ and $\rho_1^B(t_i)$ ($i = 0$ and $i = 100$) in the DFT model. A corresponding contour levels plot of $U(x, y)$ is presented in Fig. 9(a) and (b), respectively. As expected, the uncertainty region is significantly reduced at step 100.

5.2. Case II: sequential estimation with a shift in the EAW

A decision maker may change his/her attention weights during a course of sequential decisions at any time due to different reasons. These reasons may include reinforcement learning of his/her decision-making performance based on observational performance feedback, cumulative experience, and/or a significant environmental change that causes a shift on his/her

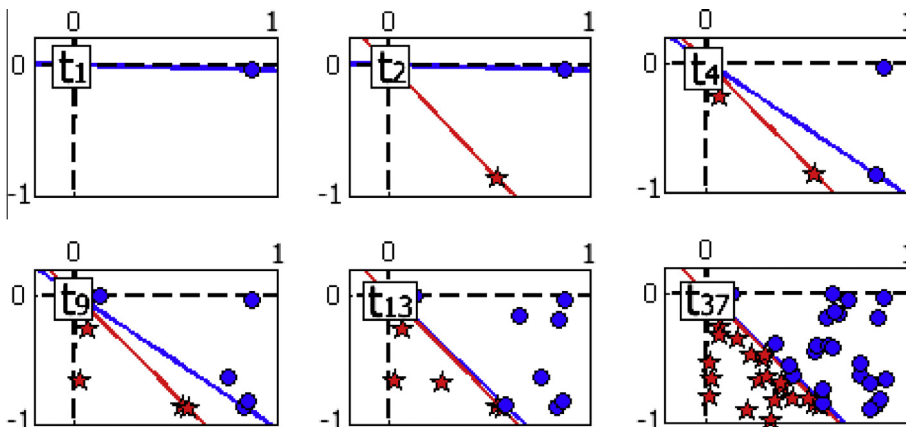


Fig. 7. Illustration of sequential estimation of DBL bounds.

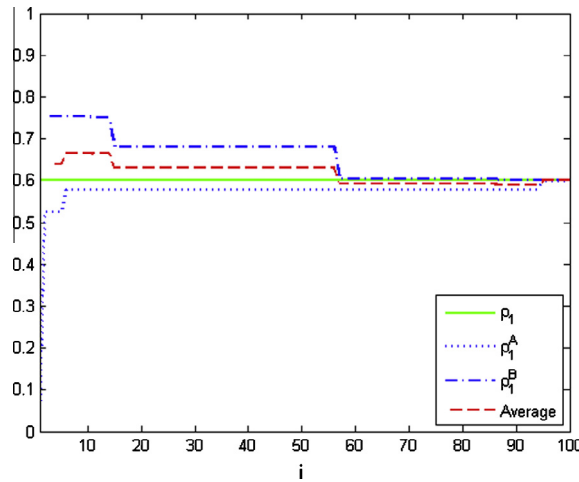


Fig. 8. Estimation bounds of the EAWs in Case I.

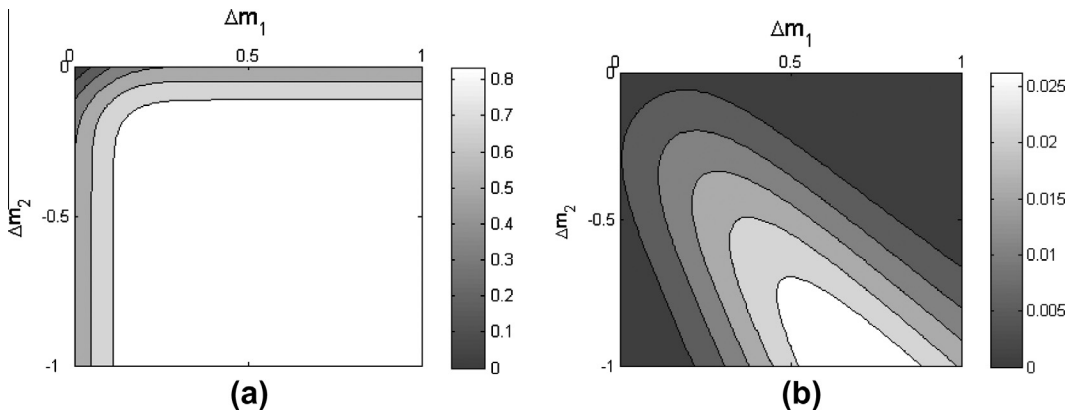


Fig. 9. $U(x,y)$ function before knowing the first decision and after decision step 100.

risk attitude or belief on alternatives. Under such a scenario with a shifting attention weight, the estimation of new EAW boundaries is adaptively adjusted by using the maximum likelihood estimation principle discussed in Section 4.6. The determination of whether an inconsistent conflict decision is due to decision uncertainty/errors or a shift of EAW, is based on the comparison of two probabilities: $P1$ in Eq. (16) and $P2$ in Eq. (17), which is given by the Justification Rule in Section 4.6.

Case II demonstrates how the proposed sequential estimation algorithm adapts to a change in the EAWs. The same simulation conditions of Case I are used in Case II, with the exception that $\rho_1(t_i)$ changes from 0.6 to 0.2 at $i = 20$. The sequential estimation procedure shown in Fig. 6 is conducted. However, in Case II the estimation of the slope bounds of DBL are re-initiated when an inconsistent decision is detected, based on the justification rule (proposed in Section 4.6). Fig. 10 shows the sequential estimation results of $\rho_1^A(t_i)$ and $\rho_1^B(t_i)$, which demonstrate the adaptive estimation capability of the proposed sequential estimation method.

5.3. Case III: human in the loop experimental tests

Case III illustrates the effectiveness of using a DFT modeling approach to characterize human decision maker’s behaviors. In this case study, real human decision samples were used. The experiment consisted of 9 sequential decision making scenarios; at each of these 9 instances, a subject was asked whether to buy stock A or stock B. The decisions were made based on two attribute values, i.e., investment safety and return, which were shown on the computer screen to the subject. The attribute values corresponding to each decision were obtained using a pre-trained Bayesian belief network (BBN) developed by Lee et al. [13]. The attributes $M(t_i)$ ($i = 1, 2, \dots, 9$) are obtained by assessing stock environmental conditions based on exogenous factors that include investment history, available fund, index increment, and previous weights. Table 1 shows

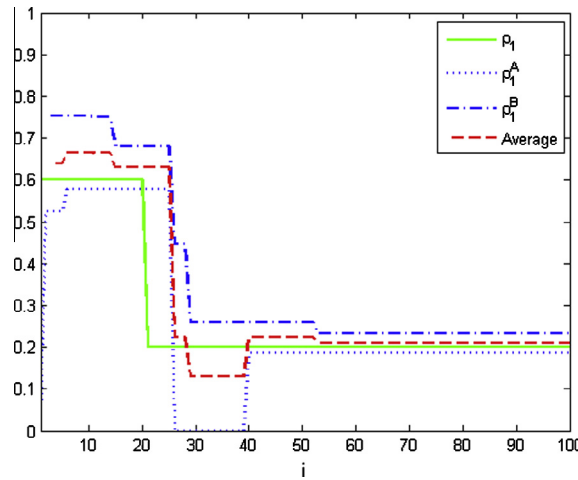


Fig. 10. Estimation bounds of the EAWs in case II.

Table 1

Attribute measurement $M(t_i)$ and the transformed value $\Delta M(t_i)$.

i	Stock A safety	Stock A return	Stock B safety	Stock B return	Δm_1	Δm_2	$\Delta m_2/\Delta m_1$
1	2.5	1.43	0.39	3.37	2.11	-1.94	-0.9194
2	3.74	1.4	0.9	3.65	2.84	-2.25	-0.7923
3	3.65	2.19	1.21	3.65	2.44	-1.46	-0.5984
4	3.12	1.4	1.46	3.17	1.66	-1.77	-1.0663
5	3.03	1.49	0.34	2.5	2.69	-1.01	-0.3755
6	3.26	1.43	1.71	3.15	1.55	-1.72	-1.1097
7	3.31	2.3	2.39	3.57	0.92	-1.27	-1.3804
8	3.01	2.11	2.33	4.04	0.68	-1.93	-2.8383
9	3.68	1.71	0.96	3.43	2.72	-1.72	-0.6324

Table 2

Estimation of DFT parameters from decisions provided by DM.

i	Provided by the subject		Estimated by sequential algorithm $b_1^B(t_i) \leq b_1 \leq b^A(t_i); \rho_1^A(t_i) \leq \rho_1 \leq \rho^B(t_i)$			
	Decision	Adjustment	b^A	b^B	$\rho_1^A(t_i)$	$\rho_1^B(t_i)$
1	Bought B	DBL ^B	0	-0.9194	0	0.4790
2	Bought B	DBL ^B	0	-0.7923	0	0.4420
3	Bought B	DBL ^B	0	-0.5984	0	0.3744
4	Bought B	-	0	-0.5984	0	0.3744
5	Bought A	DBL ^A	-0.3755	-0.5984	0.2730	0.3744
6	Bought B	-	-0.3755	-0.5984	0.2730	0.3744
7	Bought B	-	-0.3755	-0.5984	0.2730	0.3744
8	Bought B	-	-0.3755	-0.5984	0.2730	0.3744
9	Bought A	DBL ^A	-0.6324	Initiated	0.3874	Initiated

the attribute measurements and the transformed $\Delta M(t_i)$ values based on the proposed method. The decisions provided by the subject are shown in column 2 of Table 2. At each decision making instance, the EAW of a DFT model is sequentially estimated to fit the observed incoming decisions.

Based on the sequential decisions, the slope bounds b^A and b^B of DBL are sequentially estimated. Since all nine decisions are located in quadrant 4, the bounds of b^A and b^B correspond to the upper and lower bounds of the true slope b of DBL as shown in Fig. 5(a). As a result, the bounds of ρ_1^A and ρ_1^B correspond to the lower and upper bounds of the true EAW. Table 2 shows the estimation updates at each of these 9 decision trials.

Fig. 11 shows how the DBL bounds are updated based on the sampled $\Delta M(t_i)$'s. In particular, DBL^B is updated at decisions 1, 2, 3 and DBL^A is updated at decision 5. There is no inconsistent decision observed during decisions 1–8. However, a conflict point is observed at sample 9. Therefore, a further analysis is needed to justify if the subject changes his EAW at decision 9.

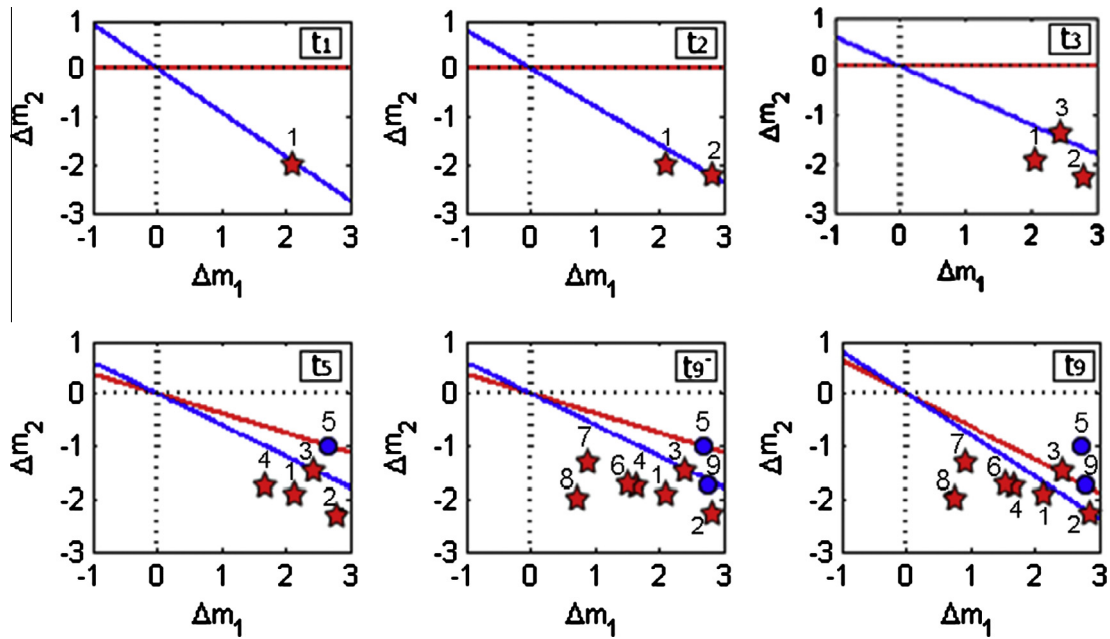


Fig. 11. Sequentially updating of DBL in Case III.

Table 3
Probability bounds for choosing alternative A based on DFT.

i	Provided by the subject Decision	Based on DFT	
		Lower probability bound	Upper probability bound
1	Bought B	0.0041	0.1058
2	Bought B	0.0130	0.2046
3	Bought B	0.0978	0.5000
4	Bought B	0.0012	0.0491
5	Bought A	0.5000	0.8844
6	Bought B	0.0008	0.0395
7	Bought B	0.0003	0.0150
8	Bought B	0.0000	0.0000

Based on the justification rule presented in Section 4.6, the probability bound $P1$ is $P1 = Prob_{[\rho_1^B(t_8)=0.3744]}^{DFT}\{choose A at point (\Delta m_1(t_9), \Delta m_2(t_9))\} = 0.4689$. In order to calculate $P2$, we assume that the EAW changes at Step 9 and a new estimation of the slope bound of DBL^A and $\rho_1^A(new)$ are obtained as $b_{new}^A = \Delta m_2(t_9)/\Delta m_1(t_9) = -1.72/2.72 = -0.6324$ and $\rho_1^A(t_9) = b^A/(b^A - 1) = 0.3874$. Based on those new bounds, an inconsistent decision is observed on decision 3. Based on (17), we have $P2 = Prob_{[\rho_1^A(new)=0.387387]}^{DFT}\{Alternative B at point (\Delta m_1(t_3), \Delta m_2(t_3))\} = 0.4695$. According to the justification rule in Section 4.6, it is concluded that the human's EAW is changed at decision 9 since $P2 > P1$. Table 3 also provides the probability bounds of all decision up step 8 based on the estimated bounds of $\rho_1^A(t_8)$ and $\rho_1^B(t_8)$. It can be seen that the advantage of using DFT model is that it can not only model human's decisions, but also can provide a quantitative probabilistic assessment of human decision's uncertainty and risk.

6. Conclusions

This paper presents a DFT modeling approach to represent the human decision maker behavior. In this approach, the human's EAWs were considered as the key parameters of the DFT model to be estimated. This estimation was performed to fit the DFT model by matching the predicted decisions using DFT with the decisions made by a human decision maker. It is shown that a linear decision boundary can be found if the EAW of the decision maker is assumed to be constant across decisions. A probability-based justification rule is provided in the paper to determine if an inconsistent decision is due to a change in the EAWs or due to intrinsic modeling uncertainty. Moreover, a sequential estimation/updating algorithm is pro-

posed to obtain the estimation bounds of the EAWs. Two simulations were conducted to demonstrate the effectiveness of the proposed algorithm under two distinct scenarios corresponding to constant and varying EAWs respectively. Furthermore, a real case study was conducted via a human in the loop experiment, which demonstrated the effectiveness of the DFT modeling approach in characterizing the human's decision making behaviors.

7. Future work

Future research is needed to extend this work to a more general decision making scenario consisting of more than two alternatives and based on more than two attributes. In a n -alternatives scenario, we should consider n different ΔM plane's, each corresponding to the comparison of one of the n alternatives with respect to the other $n - 1$. In each ΔM plane, the decision boundary is used to indicate which alternative should be chosen. With respect to the multi-attribute two-alternative scenario, a hyper plane can be used as a high dimensional linear classifier to represent the decision boundary. These same ideas may be further extended to a generalized scenario consisting of multiple alternatives. These two tasks are on-going research for our next paper

Another interesting future direction is to investigate a general decision rule by considering the decision threshold on the preference state as an unknown parameter in the DFT mode. In this situation, the decision threshold should be estimated simultaneously in parallel with the attribute weights.

Acknowledgements

This work was supported by the Air Force Office of Scientific Research under AFOSR/MURI F49620-03-1-0377.

References

- [1] J.R. Busemeyer, A. Diederich, Survey of decision field theory, *Math. Soc. Sci.* 43 (2002) 345–370.
- [2] S.H. Chew, W.S. Waller, Empirical tests of weighted utility theory, *J. Math. Psychol.* 30 (1986) 55–72.
- [3] A. Diederich, Decision making under conflict: decision time as a measure of conflict strength, *Psychon. Bull. Rev.* 10 (2003) 167–176.
- [4] A. Diederich, MDFT account of decision making under time pressure, *Psychon. Bull. Rev.* 10 (2003) 157–166.
- [5] A. Diederich, J.R. Busemeyer, Conflict and the stochastic-dominance principle of decision making, *Psychol. Sci.* (1999) 353–359.
- [6] I.E. Dror, J.R. Busemeyer, B. Basola, Decision making under time pressure: an independent test of sequential sampling models, *Memory Cognit.* 27 (1999) 713–725.
- [7] R.O. Duda, P.E. Hart, D.G. Stork, *Pattern Classification*, Wiley-Interscience, 2001.
- [8] J. Gao, J.D. Lee, Extending the decision field theory to model operators' reliance on automation in supervisory control situations, *IEEE Trans. Syst. Man Cybern. Part A Syst. Hum.* 36 (2006) 943.
- [9] J. Gao, J.D. Lee, Y. Zhang, A dynamic model of interaction between reliance on automation and cooperation in multi-operator multi-automation situations, *Int. J. Ind. Ergon.* 36 (2006) 511–526.
- [10] F.P. Gibson, M. Fichman, D.C. Plaut, Learning in dynamic decision tasks: computational model and empirical evidence, *Organ. Behav. Hum. Decis. Process.* 71 (1997) 1–36.
- [11] C. González-Vallejo, Making trade-offs: a probabilistic and context-sensitive model of choice behavior, *Psychol. Rev.* 109 (2002) 137–155.
- [12] C. González-Vallejo, A.A. Reid, J. Schiltz, Context effects: the proportional difference model and the reflection of preference, *J. Exp. Psychol. Learn. Mem. Cogn.* 29 (2003) 942–953.
- [13] S. Lee, Y.J. Son, J. Jin, Decision field theory extensions for behavior modeling in dynamic environment using Bayesian belief network, *Inf. Sci.* (2008).
- [14] S.W. Link, R.A. Heath, A sequential theory of psychological discrimination, *Psychometrika* 40 (1975) 77–105.
- [15] I.J. Myung, The importance of complexity in model selection, *J. Math. Psychol.* 44 (2000) 190–204.
- [16] R. Ratcliff, A theory of memory retrieval, *Psychol. Rev.* 85 (1978) 59–108.
- [17] J. Rieskamp, The probabilistic nature of preferential choice, *J. Exp. Psychol. Learn. Mem. Cogn.* 34 (2008) 1446.
- [18] R.M. Roe, J.R. Busemeyer, J.T. Townsend, Multialternative decision field theory: a dynamic connectionist model of decision making, *Psychol. Rev.* 108 (2001) 370–392.
- [19] H. Talaat, B. Abdulhai, *Modeling Driver Psychological Deliberation During Dynamic Route Selection Processes*, 2006, pp. 695–700.
- [20] J.T. Townsend, J.R. Busemeyer, *Approach-Avoidance: Return to Dynamic Decision Behavior*, Lawrence Erlbaum Assoc Inc., 1987, p. 107.
- [21] D. Vickers, *Decision Processes in Visual Perception*, Academic Press, 1979.